Naval Surface Warfare Center, Carderock Division

West Bethesda, Maryland 20817-5700

NSWCCD-TR-64--97/19 December 1997

Survivability, Structures, and Materials Directorate
Research and Development Report

Dielectric Materials Containing Conducting Wires: Effect on Polarization

NSWCCD--TR-64-97/19

Dielectric Materials Containing Conducting Wires: Effect on Polarization

by

Herbert Überall

REPORT DOCUMENTATION PAGE			Form Approved OMB No. 0704-0188

1. AGENCY USE ONLY *(Leave blank)*	2. REPORT DATE December 1997	3. REPORT TYPE AND DATES COVERED Final

4. TITLE AND SUBTITLE Dielectric Materials Containing Conducting Wires: Effect on Polarization	5. FUNDING NUMBERS
6. AUTHOR(S) Herbert Uberall	
7. PERFORMING ORGANIZATION NAME(S) AND ADDRESS(ES) Naval Surface Warfare Center Carderock Division 9500 MacArthur Boulevard West Bethesda, MD 20817-5700	8. PERFORMING ORGANIZATION REPORT NUMBER NSWCCD-TR-64-97/19
9. SPONSORING/MONITORING AGENCY NAME(S) AND ADDRESS(ES)	10. SPONSORING/MONITORING AGENCY REPORT NUMBER
11. SUPPLEMENTARY NOTES	
12a. DISTRIBUTION/AVAILABILITY STATEMENT Approved for public release; distribution is unlimited.	12b. DISTRIBUTION CODE

13. ABSTRACT *(Maximum 200 words)*

It has become of recent interest to complement electromagnetic responses in intensity by the additional consideration of their polarizations. In order to affect the latter, media have been considered that contain inclusions of randomly distributed and oriented short, thin wires (needles), whose polarized scattering amplitudes can modify the well-known polarization of surface reflections that is governed simply by the so-called Fresnel coefficients. In the present study, we analytically obtain, for the case of a multiplicity of perfectly conducting wires imbedded in a dielectric, the corresponding wave scattering amplitudes and their superposition with the specularly surface-reflected wave amplitude when both are being generated by the same incident wave. This allows a calculation of the total returned-wave polarizations which we express by the real Stokes parameters.

14. SUBJECT TERMS Dielectric Materials; Polarization; Reflected Wave Amplitude; Scattered Wave; Refracted Wave Amplitude			15. NUMBER OF PAGES 24
			16. PRICE CODE
17. SECURITY CLASSIFICATION OF REPORT UNCLASSIFIED	18. SECURITY CLASSIFICATION OF THIS PAGE UNCLASSIFIED	19. SECURITY CLASSIFICATION OF ABSTRACT UNCLASSIFIED	20. LIMITATION OF ABSTRACT SAR

NSN 7540-01-280-5500

Standard Form 298 (Rev. 2-89)
Prescribed by ANSI Std. Z39-18
298-102

Blank Pages

Contents

Figures

ABSTRACT

It has become of recent interest to complement electromagnetic responses in intensity by the additional consideration of their polarizations. In order to affect the latter, media have been considered that contain inclusions of randomly distributed and oriented short, thin wires (needles), whose polarized scattering amplitudes can modify the well-known polarization of surface reflections that is governed simply by the so-called Fresnel coefficients. In the present study, we analytically obtain, for the case of a multiplicity of perfectly conducting wires imbedded in a dielectric, the corresponding wave scattering amplitudes and their superposition with the specularly surface-reflected wave amplitude when both are being generated by the same incident wave. This allows a calculation of the total returned-wave polarizations which we express by the real Stokes parameters.

ADMINISTRATIVE INFORMATION

Professor Überall conducted this investigation under the auspices of the American Society of Engineering Educators (ASEE). The ASEE program at the Carderock Division, Naval Surface Warfare Center is administered by F. Halsall, Code 0112. The purpose of the continuing effort is to study the fundamental interactions of materials and electromagnetic energy.

INTRODUCTION

The reflected return of electromagnetic waves from dielectric[1,2] (including lossy ones) or metallic surfaces[3] is well-known, and can be analytically expressed by the Fresnel coefficients[1,4] which also describe the refracted wave that penetrates into the medium. These expressions are valid for infinite homogeneous, isotropic media with plane surfaces that are smooth compared to the wavelength. These expressions also describe the polarization of the reflected and refracted waves. If the polarization (electric) vector of the incident wave is perpendicular to the plane of incidence (this case termed "r"), the same will hold for the reflected and refracted waves. For the incident polarization vector that is parallel to the plane of incidence (case termed "ℓ"), reflected and refracted wave polarization vector will be parallel to the plane of incidence. Thus no coupling of linear polarizations occurs. For the ℓ-case, the reflected wave vanishes at the Brewster angle of incidence, so that for a plane incident wave of mixed polarization, the reflected wave is of purely r-type at that angle.

One may attempt to modify the polarization of waves reflected at the surface of a dielectric (which may be lossy), by imbedding short, thin wires (needles) in it that are randomly distributed and oriented. Our previous study[5] has considered such media for the case of inclusions that are small compared to the wavelength; for that case, one was able to use "effective medium theory"[6] which represents the material as one homogeneous medium with effective properties. In the present case, we chose to consider wires long compared to the wavelength (and also long compared to their diameter), so that effective medium theory is no longer applicable. The corresponding scattering cross section of one wire can be obtained from Reference 4, and the scattered wave combines coherently with the surface-reflected wave (given by the corresponding Fresnel coefficient), both being generated by the same incident wave. The effects of randomly distributed multiple wires can, however, be added together incoherently as shown by van de Hulst[7]. Polarization of the scattered wave is purely of ℓ-type and thus adds to the ℓ-type Fresnel reflection while the r-type Fresnel reflection is not affected by the wire scattering. The total ℓ-type response (reflected and scattered) is found to be superposed with different phases, rendering its amplitude complex so that the return polarization cannot be advantageously described by the customary simple polarization formula (difference of r and l amplitudes divided by their sum), which would now become complex. Instead, we characterize polarizations by the real components of the Stokes 4-vector,[7] of which only the first two are non-vanishing since only linear polarizations are involved here. Numerical calculations show the influence of scattering from the imbedded wires on the polarization of the total (reflected and scattered) returns.

REFLECTED AND REFRACTED WAVES

We consider a half space (which later on will be assumed to have a finite-size surface area A) filled with a (possibly lossy) dielectric that contains a total of N randomly distributed, randomly oriented, perfectly conducting cylindrical needles of length $l=2h$ and diameter 2a, with $a \ll h$. (Later on, these needles can be taken as being of finite conductivity and permittivity, which may be the subject of a subsequent analysis). In practice, the half space will have a finite depth, and N is the number of needles contained in its volume (A x depth).

The physical situation is as shown in Fig. 1. The wave $\mathbf{E} = \mathbf{E}_o \exp i\mathbf{k}\cdot\mathbf{r}$ is incident from below (at angle ϑ_i) through a medium with permittivity ε and permeability μ (we shall always take the case $\mu = 1$), considered to be air. The dielectric half space (top) has permittivity ε' and permeability μ' (again $\mu'=1$) and contains an upgoing refracted wave $\mathbf{E}'$ (at angle ϑ_r) while also generating a downgoing reflected wave **E″** (at angle ϑ_i). The various waves, electric vectors **E** and propagation vectors **k** are indicated in the figure.

The needle scattering of the refracted wave **E′**, which is also indicated in Fig. 1, will be discussed in the following section. At this time, we shall complete the discussion of the refracted and reflected waves shown in Fig. 1. The polarization of the incident wave is assumed to be purely linear, and we shall distinguish the two cases $\mathbf{E}_r$ and $\mathbf{E}_\ell$ as indicated in Fig.1. These amplitudes are designated as E_o^r or E_o^ℓ, while the phase factor of the incident wave is exp ($i\mathbf{k}\cdot\mathbf{r}$). As mentioned before, an incident polarization $\mathbf{E}_r$ generates $\mathbf{E}'_r$ and $\mathbf{E}''_r$ only, and an incident $\mathbf{E}_\ell$ generates $\mathbf{E}'_\ell$ and $\mathbf{E}''_\ell$ only, see Ref. 1. For the refracted amplitudes E_o' and reflected amplitudes E_o'', one has[1] as expressed in terms of the Fresnel coefficients F_{refr} and F_{refl}, respectively:

$$E_o'^{\,r,\ell} = F_{refr}^{\;r,\ell} E_o^{r,\ell} \tag{1a}$$

$$E_o''^{\,r,\ell} = F_{refl}^{\;r,\ell} E_o^{r,\ell} \tag{1b}$$

The indices of refraction are $n = (\mu\varepsilon)^{1/2}$ and $n' = (\mu'\varepsilon')^{1/2}$, and the propagation vectors have the magnitudes

$$|\mathbf{k}| = |\mathbf{k}''| = k = (\omega/c)\,(\mu\varepsilon)^{1/2} = n\omega/c \tag{2a}$$

$$|\mathbf{k}'| = k' = (\omega/c)\,(\mu'\varepsilon')^{1/2} = n'\omega/c \tag{2b}$$

where ω is the angular frequency and c the light velocity in vacuum. The angles of incidence ϑ_i and of refraction ϑ_r are related by Snell's law,

$$\sin\vartheta_i / \sin\vartheta_r = k'/k = n'/n. \tag{3}$$

In terms of these quantities, the Fresnel coefficients are

$$F^r_{refr} = \frac{2n\cos\vartheta_i}{n\cos\vartheta_i + \frac{\mu}{\mu'}\sqrt{n'^2 - n^2\sin^2\vartheta_i}} \tag{4a}$$

$$F^r_{refl} = \frac{n\cos\vartheta_i - \frac{\mu}{\mu'}\sqrt{n'^2 - n^2\sin^2\vartheta_i}}{n\cos\vartheta_i + \frac{\mu}{\mu'}\sqrt{n'^2 - n^2\sin^2\vartheta_i}} \tag{4b}$$

$$F^l_{refr} = \frac{2nn'\cos\vartheta_i}{\frac{\mu}{\mu'}n'^2\cos\vartheta_i + n\sqrt{n'^2 - n^2\sin^2\vartheta_i}} \tag{4c}$$

$$F^l_{refl} = \frac{\frac{\mu}{\mu'}n'^2\cos\vartheta_i - n\sqrt{n'^2 - n^2\sin^2\vartheta_i}}{\frac{\mu}{\mu'}n'^2\cos\vartheta_i + n\sqrt{n'^2 - n^2\sin^2\vartheta_i}} \tag{4d}$$

For lossless media, all the parameters in these expressions are real and there is no problem employing the conventional formula for the polarization of the reflected wave,

$$P_{refl} = (E''^{\,r}_o - E''^{\,l}_o)/(E''^{\,r}_o + E''^{\,l}_o) \tag{5a}$$

$$= (F^r_{refl} - F^l_{refl})\,/(F^r_{refl} + F^r_{refl}) \tag{5b}$$

which in this case is a real quantity. For lossy media, however, this expression for P_{refl} would become complex and in that case it is advantageous to describe polarizations by the (real) Stokes parameter, see the following section. Also, if needle scattering is added, the amplitudes in Eq. (5a) would become complex even for lossless media, so that here a use of the Stokes parameters is indicated, as will be shown in the next section below.

SCATTERING FROM IMBEDDED WIRES

The scattering process of the refracted wave **E′** when incident on a thin wire needle imbedded in the dielectric is indicated in Fig. 1. The first thing to be noted is that a very special scattering geometry is called for in the present situation. Since the effect of wire scattering on the polarization of the reflected wave **E″** is to be investigated here, the refracted wave that after the scattering becomes $\mathbf{E}'_{sc}$ and then re-emerges from the medium as $\mathbf{E}''_{sc}$ must be such that this emerging wave $\mathbf{E}''_{sc}$ is directed parallel to the reflected wave $\mathbf{E}''$ (with $\mathbf{k}''_{sc} = \mathbf{k}''$), so that both of these (coherently interfering) waves can be observed together, and their combined polarization obtained. This forces us to consider the symmetric scattering geometry of Fig. 1 only, with scattered and re-emergence angles ϑ_r and ϑ_i as indicated, and the whole process taking place in the (xz) plane of incidence exclusively.

The geometry of scattering from a thin cylinder is defined in Reference 4, and is shown here in Figs. 2(a) and (b) in a coordinate system $(\widetilde{xyz})$. Incident and scattered waves are assumed to be directed at angles Ψ_i and Ψ_s from the cylinder normal, and the (linear) polarizations of both are here kept more general than those considered earlier in this report (r or ℓ), i.e., lying at angles γ_i (γ_s) from the plane of incidence (scattering). Our basic coordinate system (xyz), however, is as shown in Fig. 1, so that if the wire is directed at spherical angles (ϑ, φ) in that system, a coordinate transformation between the two systems is in order. This is sketched in Fig. 3(a) for the wave incident on the wire, and in Fig. 3(b) for the scattered wave. The spherical-triangle relationships then give the equations

$$\sin \Psi_i = \cos \vartheta \cos \vartheta_r + \sin \vartheta \sin \vartheta_s \cos \varphi \qquad (6a)$$

$$\sin \Psi_s = \cos \vartheta \cos \vartheta_r - \sin \vartheta \sin \vartheta_r \cos \varphi \qquad (6b)$$

which will be needed later in this calculation.

The amplitude of the refracted wave $\mathbf{E}'$ as scattered by the wire needle imbedded in the dielectric (Fig. 1), may be obtained by using the procedures outlined in the Radar Cross Section Handbook.[4] This reference only quotes the scattering cross-section (squared amplitude), but the amplitude itself (including phase) can be found in analogy to van de Hulst's derivations[7] that are based on Huygens' principle. One should note that this reference employs waves

$\exp(-ikz+i\omega t)$, so that the complex conjugate of the expressions quoted therein must be used for our purposes.

We will need the far-field scattering amplitude of the wire which at distance r behaves as a spherically spreading wave $r^{-1} e^{ik'r}$. (This is obtained here schematically since the subsequent emergence of the scattered wave from the medium will transform it into a spherical wave $r^{-1}e^{ikr}$ thereafter.) This far-field amplitude is found by van de Hulst starting from the near-field amplitude which spreads cylindrically $\propto r^{-1/2}e^{ik'r}$, and transforming it into the far-field amplitude by invoking Huygens' principle, which obtains the propagated field as a superposition of spherical wavelets that emanate from each point of the field before its propagation. Van de Hulst's result of this approach is given in Ref. 7, p. 305 as the amplitude u,

$$u = (2ih/\pi r)ET \exp(ik'r) \qquad (7)$$

where E is a strongly-peaked $x^{-1} \sin x$ - type function with side lobes, to be defined later, and T is the near-field scattering amplitude of the cylinder (which in this case may be taken as infinitely long). The choice of this amplitude is governed by the relation between cylinder radius and wavelength, and we here choose the amplitude for T given as a closed-formed expression by Ruck et al. (Ref. 4, p. 211), valid for very thin perfectly conducting cylinders ($k'a \ll 1$) in the form

$$E_{\parallel}^{sc} = E_{\parallel}(\pi/2k'r)^{1/2} [\ln(0.8905\, k'a)-i\pi/2]^{-1} \exp[i(k'r + \pi/4)] \qquad (8)$$

where the polarization is accounted for: $E_{\parallel}$ are the field components parallel to the cylinder axis. [Although Ruck refers to this expression as a "far field", it is here the cylindrically spreading field relatively close to the cylinder which in van de Hulst's approach is taken as the "near field".] The scattering amplitude resulting from the combination of Eqs. (7) and (8) is not given in Ref. 7, where only the bistatic scattering cross section σ_b is quoted. The latter is defined (by Ref. 7 and the general "engineering literature") as

$$\sigma_b = 4\pi\, d\sigma/d\Omega \qquad (9a)$$

which is written here in terms of the expression $d\sigma/d\Omega$ used in the "scientific literature":

$$d\sigma/d\Omega = r^2|E_{sc}|^2/|E_{inc}|^2 \qquad (9b)$$

The expression for σ_b may be calculated from Eqs. (7) and (8) and compared with that of Ref. 7, in order to verify (up to possible phases) the correctness of our calculation. Inserting in Eq. (9a) and noting that (cf. Fig. 2) projecting $\mathbf{E}'$ (or $\mathbf{E}'^{sc}$) on the $\widetilde{xz}$ plane (or the scattering plane) introduces factors $\cos\gamma_i$(or $\cos\gamma_s$) while the further projection on the $\tilde{z}$ axis adds factors with Ψ_i (or Ψ_s), the latter in the manner $E'^{sc}\cos\Psi_s = E'\cos\Psi_i(\ldots)$ in Eq. (8). This leads to the result

$$\sigma_b = 4\pi h^2(\cos\Psi_i/\cos\Psi_s)^2\{\sin[k'h(\sin\Psi_i + \sin\Psi_s)]/k'h(\sin\Psi_i + \sin\Psi_s)\}^2$$

$$\cdot \cos^2\gamma_i \cos^2\gamma_s / [\ln^2(0.8905\, k'a) + \pi^2/4], \qquad (10)$$

in agreement with Ref. 4, p. 304. Note that from Eq. (6), we have

$$\sin\Psi_i + \sin\Psi_s = 2\cos\vartheta\cos\vartheta_r\ . \qquad (11)$$

It should be added that in Ref. 4, Eq. (4.3-4.4) our factor $(\cos\Psi_i/\cos\Psi_s)^2$ appears upside-down, but we believe that our version is the correct one, as can be backed up by certain physical arguments. However, in our problem it will be shown below that $\Psi_s = -\Psi_i$, so that the factor in question equals unity in either version.

The peaked angular function E is now identified, using Eq. (11), as

$$E = \sin(2k'h\cos\vartheta\cos\vartheta_r)/(2k'h\cos\vartheta\cos\vartheta_r) \qquad (12)$$

With $\alpha = 2k'h \cos \vartheta_r$ and $\mu = \cos \vartheta$, this can be written as

$$E = \sin \alpha\mu / \alpha\mu \tag{13a}$$

and for the case $k'h \gg 1$, that shall interest us here, it approaches a δ-function in the variable μ:

$$\lim_{\alpha \to \infty} \sin \alpha\mu / \alpha\mu = (\pi/\alpha)\, \delta(\mu) \tag{13b}$$

indicating that scattering occurs at, or close to, $\vartheta = 0$, or from Eq. (11), at $\Psi_s = -\Psi_i$ as stated previously. From Eq. (10), one also notes that the scattering cross section is completely independent of azimuth, as noted by Ref. 4. This indicates that the scattering takes place along a thin cone, see Fig. 4. Its opening angle is the same as the angle of incidence, and the scattered field is distributed uniformly over the cone. From Eq. (8), no scattering takes place if the incident wave's electric field is perpendicular to the scattering plane; and likewise, the scattered electric field has no perpendicular component. The physical reason for these two facts is that the electric fields need to have a component along the wire in order to generate a current in it.

For the case considered by us, the width of the cone, which is $\Delta\mu = \pi / \alpha$ in angle for Eq. (13a), will be very small. As a consequence, only those wires participate in the scattering (for the geometry of Fig. 1) that are close to horizontal, and close to the plane of incidence and scattering (the xz plane). Fortunately, the scattering cone has angle $\Psi_s = -\Psi_i$ so that the scattered radiation has precisely its dominant component along $\mathbf{k}'_{sc}$ (Fig. 1) where it is needed.

As said above, the scattered field is purely ℓ-type and will add to the ℓ-type reflected field; the r-type reflected field has no addition from the scattering.

We can explicitly relate the amplitude u as obtained from Huygens' principle to the near-field scattering amplitude T, using van de Hulst's result, Ref. 7, p. 302, in order to define the phase of T when Eq. (8) is used for this amplitude. In the latter expression, we employ $\Psi_s = -\Psi_i$, as shown before, and $\gamma_i = \gamma_s = 0$ in order to obtain the scattering amplitude $E_{\parallel}^{\parallel}$. Averaging over the wire orientations in ϑ which eliminates the δ-function in Eq. (13b) and furnishes the factor (1/2) $(\pi/2k'h \cos \vartheta_r)$, we find

$$\langle E'_{sc} \rangle_\vartheta = E_o'' \pi \exp(ik'r) / \{4k'r \cos \vartheta_r [\ln(0.8905\ k'a) - i\pi/2]\} \tag{14}$$

so that we have been able to transform the cylindrically spreading field of Eq. (8) into a spherically spreading field, Eq. (14), as desired. There still remains the task of averaging this scattered field over the azimuth of the wire orientations, φ. While for the ϑ-orientations, this average was automatically taken care of by the δ-function, it has to be done here explicitly for the φ - average.

Fig. 5 shows a view into the cone opening, indicating its thickness $\Delta\vartheta = \pi/(2k'h \cos \vartheta_r)$ and since the cone axis, i.e., the wire, is horizontal, its azimuthal width Δφ. Elementary geometry furnishes $\Delta\varphi = (2\pi / k'h)^{1/2}$. A factor 2 to be inserted in the φ-average comes from the fact that wires both oriented at $\varphi = 0$ and $\varphi = \pi$ contribute to the scattering amplitude, see Fig. 1. An incoherent summation over all the N wires in the sample provides a further factor N, so that finally the scattered field doubly averaged in this way becomes

$$\langle E'_{sc} \rangle_{\vartheta,\varphi} = E_o'' \exp(ik'r)\, N(2\pi/k'h)^{1/2} / \{4k'r \cos \vartheta_r \cdot [\ln(0.8905\ k'a) - i\pi/2]\} \tag{15}$$

This field is now incident (Fig. 1) under the angle ϑ_r onto the medium boundary, coming from inside the medium and about to re-emerge into the air below. This re-emergence calls for a Fresnel refraction coefficient, inverse to that of F'_{refr} that applied to penetration from the air into the medium. This can be obtained from Eq. (4c) by simply substituting $\vartheta_i \leftrightarrow \vartheta_r$, $\varepsilon\mu \leftrightarrow \varepsilon'\mu'$ or

$n \leftrightarrow n'$, and we obtain this coefficient which we call F''_{refr} as:

$$F''_{refr} = \frac{2nn' \cos \vartheta_r}{\frac{\mu'}{\mu} n^2 \cos \vartheta_r + n'\sqrt{n^2 - n'^2 \sin^2 \vartheta_r}} \tag{16}$$

The field re-emerging into the air will thus be Eq. (15), now having k′ again converted into k by the refraction, and multiplied by the refraction coefficient of Eq. (16). This is to be added coherently to the reflected field **E″** in order to find the change of polarization of the latter caused by the wire scattering. A problem then arises, however, because the reflected field **E″** is apparently a plane wave (having been generated by the reflection of the incident plane wave from an infinite plane boundary) and the wire scattered wave, Eqs. (15) and (16), is a spherically divergent wave. Adding these two fields together would amount to comparing apples with oranges.

The answer to this lies in the fact that our sample is not of infinite size, but has a finite surface area A. For a far-distant observer, the reflected wave from this finite sample has to be a spherically divergent wave also. This wave can then consistently be added to the divergent wave of the wire scattering process; it can be obtained from the plane reflected wave again by an application of Huygens' principle.

In the coordinate system (x,y,z) of Fig. 1, the reflected wave leaving the surface equals $u_{surf} = \exp(i\mathbf{k}'' \cdot \mathbf{r})$ at z=0, apart from the amplitude factor $\mathbf{E}''_0$. The Huygens' formula for a plane starting surface is obtained by van de Hulst[7] (p. 20) as:

$$u = -(ik / 2\pi r)\, u_{surf} \exp(ikr)\, dS, \tag{17}$$

and we assume a total surface area of $A = (-d_x / 2 \leq x \leq d_x / 2, -d_y / 2 \leq y \leq d_y / 2)$. However, Eq. (17) was obtained by Ref. 7 for a surface normal to the propagation direction $\hat{k}''$, so we turn to a new coordinate system (ξ, η, ζ) as shown in Fig. 6, and use the projected area $A \cos \vartheta_i$ as the starting surface. On it, the surface value is $\tilde{u}_{surf} = \exp(-ik\,\zeta) = 1$ at $\zeta = 0$. Thus, expanding the radius factor in the exponential of Eq. (17) as $r + (\xi^2 + \eta^2) / 2r$, we get

$$u = -(ik/2\pi r)\exp(ikr) \int_{-d_x\cos\vartheta_i/2}^{d_x\cos\vartheta_i/2} d\xi \int_{-d_y/2}^{d_y/2} d\eta \exp\left[ik(\xi^2+\eta^2)/2r\right], \qquad (18)$$

or

$$u = -(2ik/\pi r)\exp(ikr)\, I_\xi\, I_\eta, \qquad (19a)$$

with

$$I_\xi = \int_0^{d_x\cos\vartheta_i/2} d\xi \exp(ik\xi^2/2r), \qquad (19b)$$

$$I_\eta = \int_0^{d_y/2} d\eta \exp(ik\eta^2/2r). \qquad (19c)$$

Using the definition of the Fresnel integrals[8]

$$C(u) = \int_0^u \cos(\pi t^2/2)dt, \qquad (20a)$$

$$S(u) = \int_0^u \sin(\pi t^2/2)dt, \qquad (20b)$$

we find

$$I_\xi = (\pi r/k)^{1/2}[C((k/\pi r)^{1/2} d_x \cos\vartheta_i/2) + i\, S((k/\pi r)^{1/2} d_x \cos\vartheta_i/2)]\,, \tag{21a}$$

$$I_\eta = (\pi r/k)^{1/2}[C((k/\pi r)^{1/2} d_y/2) + i\, S((k/\pi r)^{1/2} d_y/2)]\,. \tag{21b}$$

For the case considered by us, i.e., for distant observers, u is small and one has

$$C(u) \cong u\,, \tag{22a}$$

$$S(u) = O(u^3)\text{ , i.e., negligible,}$$

leading to the answer

$$u \cong -(ik^2/2\pi kr)(A \cos \vartheta_i) \exp(ikr)\,. \tag{23a}$$

This is indeed a spherically spreading wave as desired, that can be added to Eq. (15) multiplied by Eq. (16); here Eq. (23a) must be supplemented by the factor (Fig. 1):

$$\mathbf{E}_o''^{\ell} \equiv F^{\ell}_{refl}\, E_o \hat{E}_o''^{\ell} \tag{23b}$$

TOTAL FIELDS

From all the foregoing, we now have the total fields as seen by an observer at large distance r(carets denoting unit vectors):

(a) perpendicular case (r):

$$\mathbf{E}^r_{tot} \equiv \mathbf{E}^r_{refl} = E_o \hat{E}_o''^{\,r} F^r_{refl} (-ik^2/2\pi kr)\, (A \cos \vartheta_i) \exp(ikr) \tag{24a}$$

(b) parallel case (ℓ):

$$\mathbf{E}^{\ell}_{tot} = E_o \hat{E}_o''^{\,\ell} F^{\ell}_{refl} (-ik^2/2\pi kr)\, (A \cos \vartheta_i) \exp(ikr)$$

$$+ E_o \hat{E}_o''^{\,\ell} F^{\ell}_{refl} F''^{\ell}_{refl} (2\pi/k'h)^{1/2} (N/4kr \cos \vartheta_r)\, [\ln(0.8905\, k'a) - i\pi/2]^{-1}$$

$$\cdot \exp(ikr). \tag{24b}$$

POLARIZATIONS

As stated above, the correct way of characterizing polarizations is via the use of the (real) Stokes parameters I, Q, U, and V. These are defined as[7]

$$I = E_\ell E_\ell^* + E_r E_r^* = \text{intensity (energy flux/area)},$$

$$Q = E_\ell E_\ell^* - E_r E_r^*$$

$$U = E_\ell E_r^* + E_r E_\ell^* \qquad (25)$$

$$V = i\,(E_\ell E_r^* - E_r E_\ell^*)$$

which may be combined into the Stokes 4-vector

$$S = \begin{pmatrix} I \\ Q \\ U \\ V \end{pmatrix} \qquad (26)$$

If only linear polarizations are involved, as is the case here, one has U = V = 0.

An incident wave that is purely linear parallel polarized, has

$$S^\ell = E_0^2 \begin{pmatrix} 1 \\ 1 \\ 0 \\ 0 \end{pmatrix} \qquad (27a)$$

or if purely perpendicular,

$$S^r = E_0^2 \begin{pmatrix} 1 \\ -1 \\ 0 \\ 0 \end{pmatrix} \qquad (27b)$$

For the scattered/re-emerging wave, one may define

$$F^{r,\ell}_{refl} = |F^{r,\ell}_{refl}| \exp i\Psi^{r,\ell}_{refl}$$

$$F^{\ell}_{refr} = |F^{\ell}_{refr}| \exp i\Psi^{\ell}_{refr} \tag{28}$$

$$F''^{\ell}_{refr} = |F''^{\ell}_{refr}| \exp i\Psi''^{\ell}_{refr}$$

(for a possibly lossy medium), and

$$\chi = \tan^{-1} [(\pi/2)/\ln (0.8905\ k'a)]; \tag{29}$$

further,

$$B^{\ell}_{refl} = |F^{\ell}_{refl}|\ (k^2/2\pi)\ A \cos \vartheta_i,$$

$$\varepsilon^{\ell}_{refl} = \Psi^{\ell}_{refl} - \pi/2, \tag{30}$$

$$B^{\ell}_{sc} = |F^{\ell}_{refr} F'^{\ell}_{refr}|\ (2\pi/k'h)^{1/2}\ (N/4 \cos \vartheta_r)[\ln^2(0.8905\ k'a) + \pi^2/4]^{-1/2},$$

$$\varepsilon^{\ell}_{sc} = \chi + \Psi^{\ell}_{refr} - \Psi''^{\ell}_{refr} \tag{31}$$

This yields the Stokes parameters (disregarding the overall factor $1/k^2r^2$):

(a) perpendicular case (r):

$$I_r = -Q_r = E_o^2\ |F^{r}_{refl}|^2 (k^2\ A \cos \vartheta_i/2\pi)^2, \tag{32a}$$

(b) parallel case (ℓ):

$$I_\ell = Q_\ell = E_o^2\ \{(B^{\ell}_{refl} \cos \varepsilon^{\ell}_{refl} + B^{\ell}_{sc} \cos \varepsilon^{\ell}_{sc})^2 + (B^{\ell}_{refl} \sin \varepsilon^{\ell}_{refl} + B^{\ell}_{sc} \sin \varepsilon^{\ell}_{sc})^2\} \tag{32b}$$

These equations are amenable to numerical calculations in a straightforward manner.

CONCLUSIONS

We have calculated intensities and polarizations of an electromagnetic wave returned from a flat, smooth, dielectric sample of surface area A that contains a total of N randomly positioned and randomly oriented, perfectly conducting needles. The returns consist, for an incident wave polarized linearly and perpendicularly to the plane of incidence, of a reflected wave only with the same perpendicular polarization. For parallel polarization, the return has both a reflected and a wire-scattered component. The peculiar scattering geometry of a perfectly conducting wire (in the form of a thin-walled cone) introduces strong reductions in scattering intensity due to the fact that only few wire needles satisfy this geometry. However, lesser geometrical restrictions can be expected for a (lossy) dielectric wire, with a corresponding improvement in scattered intensity. We have here considered the case of wires long compared to the wavelength, utilizing the appropriate scattering amplitude of Eq. (8). In a different frequency regime, our formalism is sufficiently flexible to permit its replacement by a different appropriate expression for the scattering amplitude, including one corresponding to a (lossy) dielectric wire if desired.

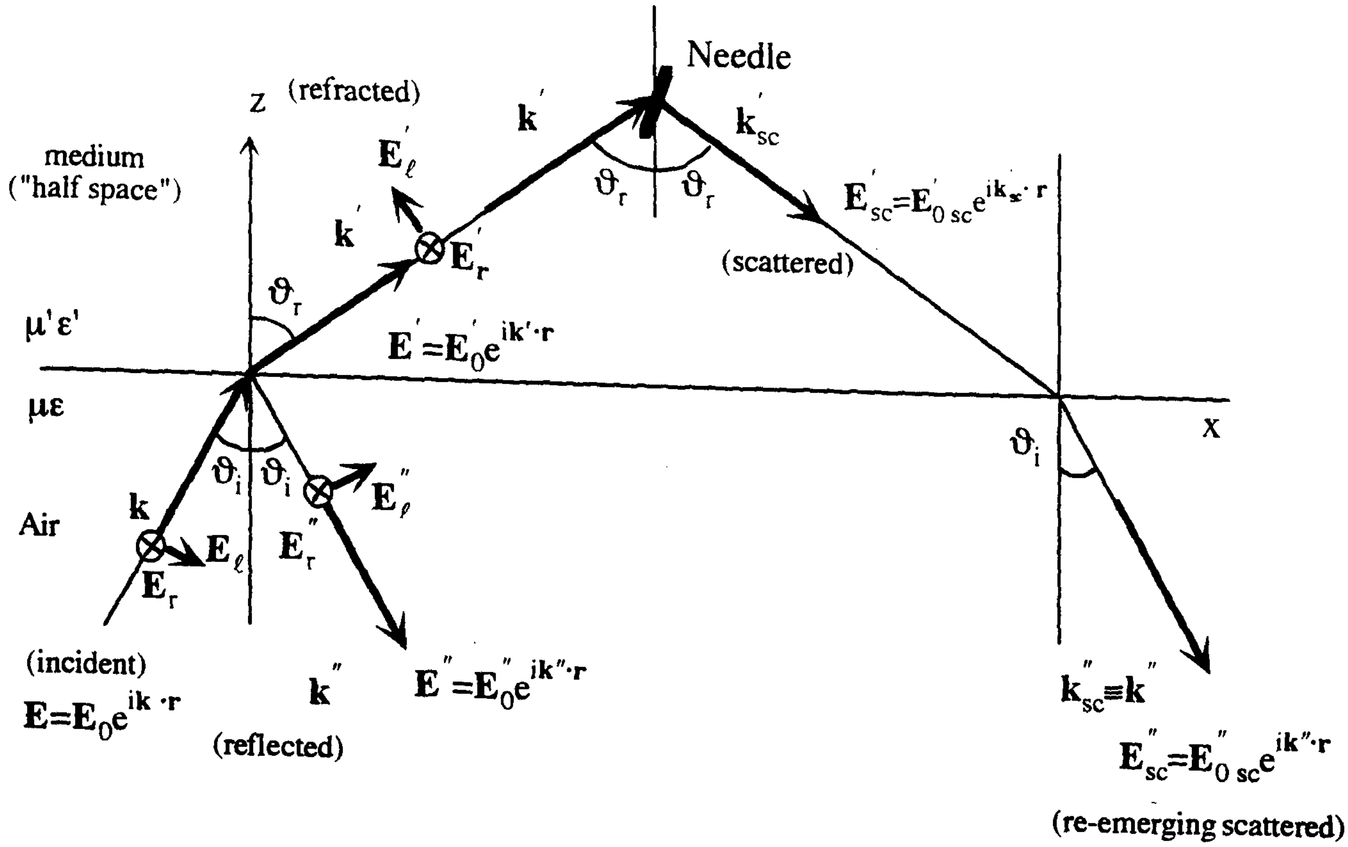

Figure 1. Geometry of reflection, refraction, and needle scattering/re-emergence of waves.

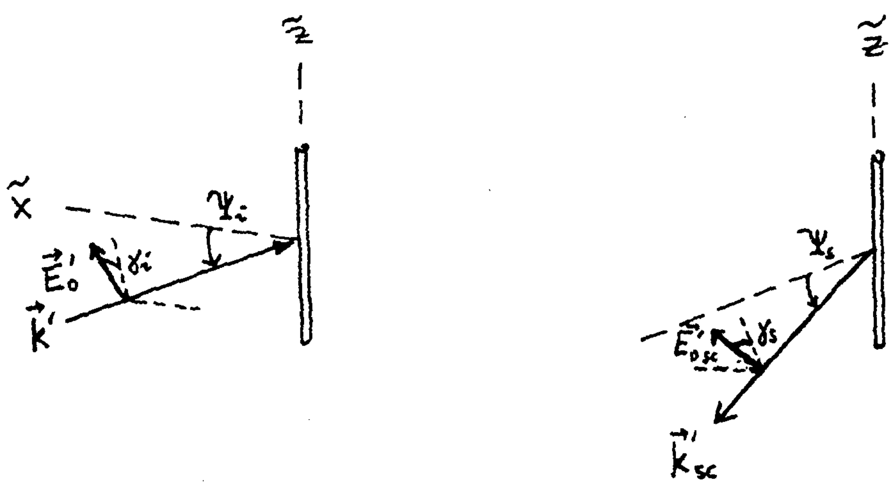

(a)

(b)

Figure 2. Geometry of incidence on (a), and scattering from (b) a thin cylinder.

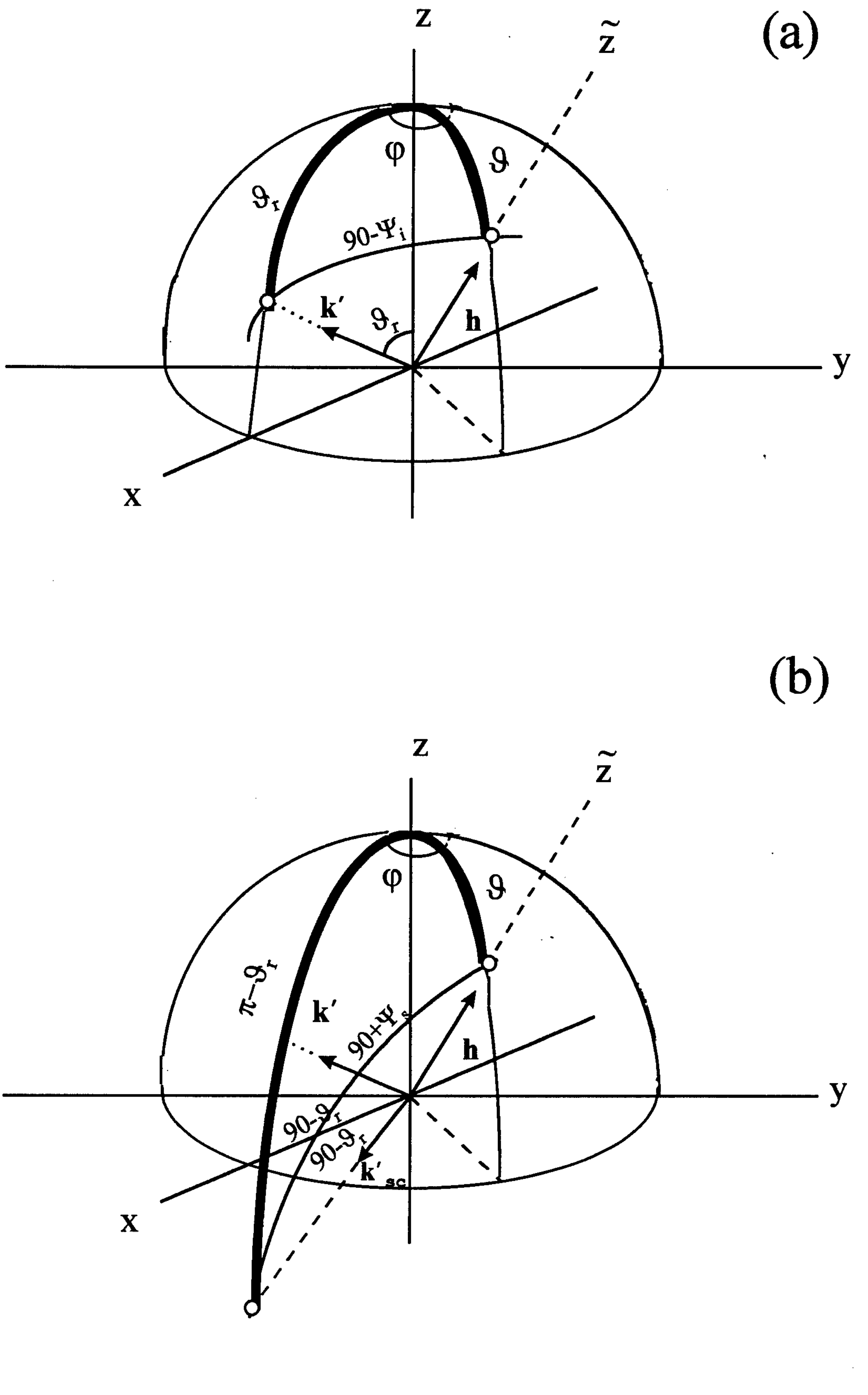

Figure 3. Geometry of incidence on wire **h** (a), and of the scattering from it (b).

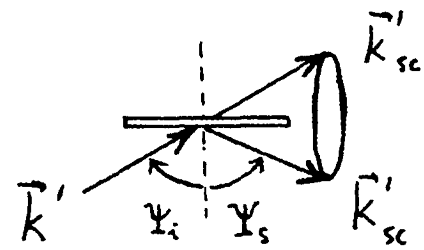

Figure 4. Conical scattering from a thin, perfectly conducting wire.

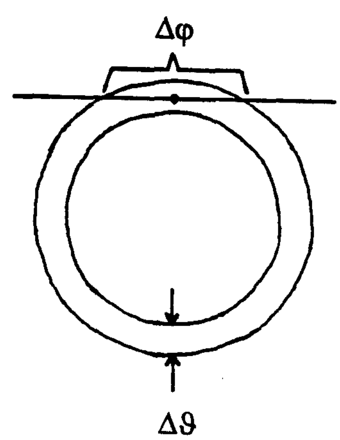

Figure 5. Vertical and azimuthal widths (Δϑ, Δφ) of the scattering cone.

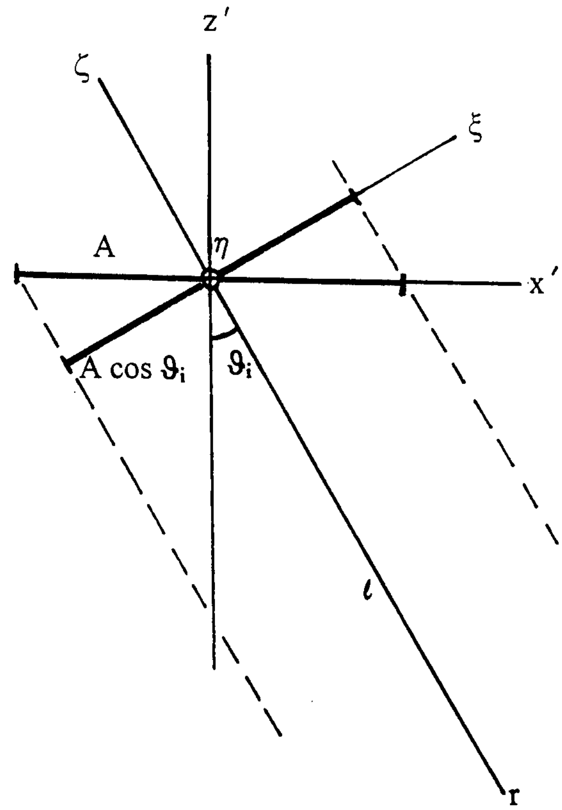

Figure 6. Coordinate system for the reflected wave spherically divergent from a sample of surface area A, in order to obtain that wave using Huygens' principle.

REFERENCES

1. Jackson, J.D., Classical Electrodynamics (2nd ed.), Wiley, New York (1975).

2. Stratton, J.A., Electromagnetic Theory, McGraw Hill, New York (1941).

3. Born, M. and E. Wolf, Principles of Optics (4th ed.), Pergamon, New York (1952).

4. Ruck,G.T., D.E. Barrick, W.D. Stuart, and C.K. Krichbaum, Eds., Radar Cross Section Handbook, Plenum, New York (1970).

5. Überall, H., B.F. Howell, and E.L. Diamond, "Effective Medium Theory and the Attenuation of Graphite Fiber Composites," J.Appl. Phys., Vol. 73, pp. 3441-3445 (1993).

6. Aspnes, D.E., "Optical Properties of Thin Films," Thin Solid Films, Vol. 89, pp. 249-262 (1982).

7. van de Hulst, H.C., Light Scattering by Small Particles, Dover, New York (1957).

8. Morse, P.M., and H. Feshbach, Methods of Theoretical Physics, McGraw Hill, New York (1953).

INITIAL DISTRIBUTION

Name	Copies
CHIEF OF NAVAL RESEARCH BALLSTON CENTRE TOWER ONE 800 NORTH QUINCY ST ARLINGTON VA 22217-5660 ATTN CODE 332 POHANKA	1
CHIEF OF NAVAL RESEARCH BALLSTON CENTRE TOWER ONE 800 NORTH QUINCY ST ARLINGTON VA 22217-5660 ATTN CODE 332 SEDRIKS	1
CHIEF OF NAVAL RESEARCH BALLSTON CENTRE TOWER ONE 800 NORTH QUINCY ST ARLINGTON VA 22217-5660 ATTN CODE 333 LEKOUDIS	1
CHIEF OF NAVAL RESEARCH BALLSTON CENTRE TOWER ONE 800 NORTH QUINCY ST ARLINGTON VA 22217-5660 ATTN CODE 361 LINDER	1
JOHNS HOPKINS UNIVERSITY MATERIALS SCIENCE DEPARTMENT CHARLES AND 34TH STREET BALTIMORE MD 21218 ATTN DR JOSEPH DICKEY	2
DEFENSE TECHNICAL INFORMATION CENTER 8725 JOHN KINGMAN ROAD SUITE 0944 FORT BELVOIR VA 22060-6218	1

CARDEROCK DIVISION

Code	Name	Copies
0112	Douglas	1
3442	TIC	1
64	Fischer	2
641		1
642		25
683	Bardo	1
70		1
72		1
722		1
723		1
80		1